ISBN: 978-984-34-8313-3
www.iabse-bd.org

Mapping river bathymetry using Stumpf model

A. Akter & A. Dayem
Chittagong University of Engineering & Technology (CUET), Chittagong 4349, Bangladesh.

ABSTRACT: River bathymetry maps are the prerequisite for any river engineering and management projects. Traditionally, river bathymetry mapping is carried out using an echo sounder instrument, and this practice involves both time and costs. The process faces challenges with inaccessible water regions, thus, adapting remote sensing technology seems to be an alternate solution. This study aimed to determine Karnaphuli river bathymetry using the Stumpf model based on the ratio transform algorithm for the selected years. Then, eroded and deposited areas within the Karnaphuli river were identified. Riverbank line Landsat images for the selected years were analyzed and 21 observation points were identified for further investigations. Thus, this study envisages as a basis to develop river bathymetry maps using geospatial techniques once ground-truthing is available.

1 INTRODUCTION

Bathymetry mapping is the prime consideration for river restoration as well as to establish a sustainable river health. To acquire detailed knowledge on sedimentation and siltation, bathymetry mapping is required for near coasts, harbors, near shoals, and river banks (Tripathi and Rao, 2002; Jawak, Raut and Luis, 2015; Pushparaj and Hegde, 2017). River bathymetry usually acquired through a hydrographic survey and also application of geospatial technology (Deng, Ji and Zhang, 1979; Winterbottom and Gilvear, 1997). Compare to the Ultrasonic sonar-based hydrographic survey; the remote sensing process requires satellite images of multiband high resolution to acquire the water depth. To conduct a dynamic hydrographic survey, satellite-based image processing is updating with recent improved empirical and analytical algorithms (Lyzenga, 1978; Stumpf et al., 2003; Lyzenga, Malinas and Tanis, 2006; Su, Liu and Heyman, 2014; Abd-almajied, 2015). To date, researchers have reasonably applied satellite or airborne data for water depth acquisition from rivers and seas(Benny and Dawson, 1983; Cracknell and Ibrahim, 1988). Water depth estimation using remote sensing data depends on the available amount of reflected light, water clarity, water depth attenuation, bottom reflectance and scattered suspended solids (Baban, 1993)(Abd-almajied, 2015).This study aimed to achieve bathymetry maps through water depth prediction using spectral reflectance through shallow to deep water. In this connection, Landsat-8 images were used for satellite-derived bathymetry mapping. A Global Positioning System (GPS) based echo-sounding survey was conducted to acquire bathymetry maps for the Karnaphuli River.

2 STUDY AREA

Karnaphuli River (between 22°12'60.00" N and 91°47'59.99" E), originated from Lushai hills in Mizoram state of India, is one of the most important and largest rivers for the Chittagong city and the Chittagong hill tracts, With a total length of 180 km steep waterway passes Rangamati at a confined loop and progresses as a zigzag course towards two more prominent loops in the Dhuliachhari and the Kaptai (Figure 1). Starting from the Kaptai loop, the river meandering covers Sitapahar hill range and, thus, flows across the plain of Chittagong through Chandraghona hills and finally drains into the Bay of Bengal (Figure 1).

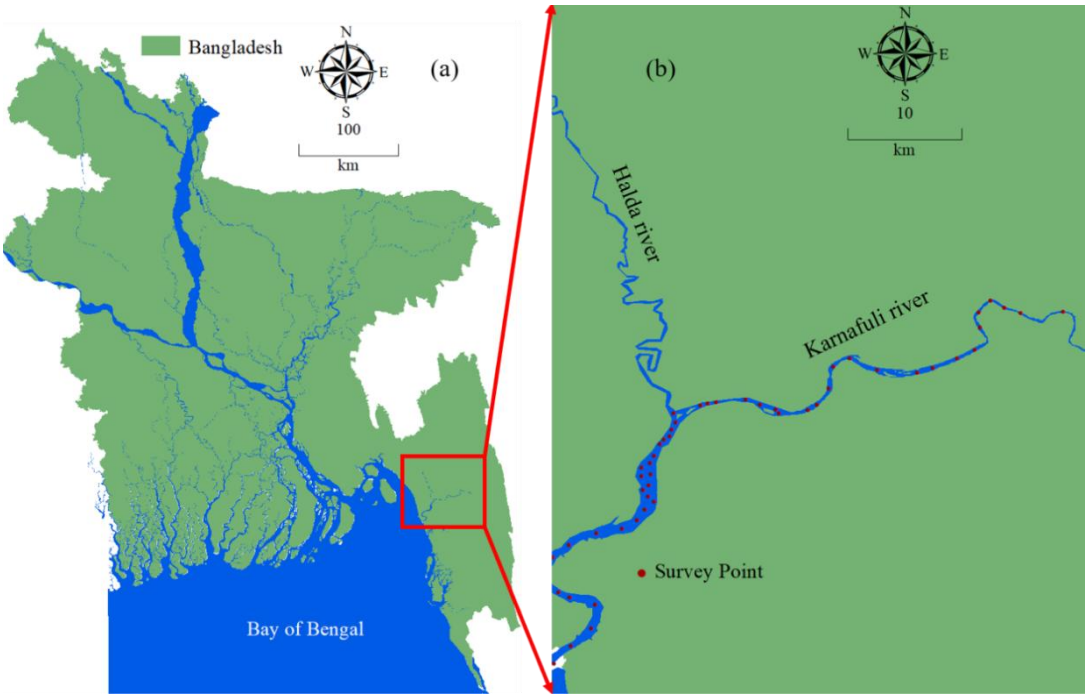

Figure 1. Bangladesh (left) (USGS, 2014 (left) and Karnaphuli river prepared by adopting NDWI (right).

3 DATA SOURCE AND PREPARATION

An attempt was made to satellite-derived bathymetry mapping of the study area for a different time interval from 1978 to 2018. In this study, the processing of Blue and Green bands of Landsat-8 imagery was selected (Table 1). The blue band radiance range (450-515nm) is lower with low water depth compared to the Green band (526-600nm). On the other hand, in the field survey, a set of 50 uniformly distributed points were considered for water depth survey using echo-sounder.

Table 1. Landsat data information.

Sensor	Year	Acquisition Date	Path	Row
MSS (Multispectral Scanner System)	1978	15 April 1978	146	44
		1 March 1978	145	44
Landsat-4	1985	18 May 1985	136	45
		18 May 1985	136	44
Landsat-4	1999	12 March 1999	136	45
		12 March 1999	136	44
Landsat-5	2011	27 February 2011	136	45
		27 February 2011	136	44
Landsat-8	2018	11 October 2018	136	45
		11 October 2018	136	44

Satellite-based Landsat remotely sensed imagery is usually affected by the atmospheric particles, these include water vapor, gases, dust. Mie scattering affects the earth's surface reflectance because the lower portions of the atmosphere are filled by the larger particles i.e. water vapor, dust, and pollen (El-sayed, 2018). Process atmospheric correction process might eliminate the lower atmospheric effects (El-sayed, 2018). To prepare river water depth maps from Landsat imagery using geospatial based techniques involved atmospheric correction and geometric correction. In this context, visible wavelengths were processed and thus reduction of reflected radiation or emission from the earth surface could achieve. In this phase, the digital numbers of the imagery were converted into uncontaminated atmosphere reflectance using metadata with USGS equations (Eq.1) (El-sayed, 2018). These reflectance values significantly represent surface actual reflectance, used to Universal Transverse Mercator(UTM) projection and the WGS84 datum.

$$P_\lambda = \frac{\pi L_\lambda d^2}{ESUN_\lambda \sin\theta} \quad (1)$$

Where, P_λ = Surface and atmospheric reflectance.

L_λ = Radiance in units of W / (m^2. sr .µm)
D = Earth-sun distance, in astronomical units.
$ESUN_\lambda$= Solar irradiance in units of W / (m^2µm)
θ = Sun elevation (⁰)

4 METHODOLOGY

Initially, satellite imagery was collected for the study area in an optimal environmental condition. Then, these images were processed for the atmospheric and geometric corrections. Then to estimating river bathymetry, the processed images were visualized in ESRI ArcMap software ver. 10.5 and 3D Analyst Tool. River water depth acquisition from Landsat images was conducted based on the principle of light attenuates exponentially in the river water. In this study, the well-known Stumpf model was used. The Stumpf model or 'Log-Ratio model' (Stumpf *et al.*, 2003)(Duplančić, Leder and Peroš, 2019), follows the fundamentals of water absorptivity and varies spectrally among image bands (Eq.2). Stumpf model working equation is:

$$Z = m_1 \frac{\ln(nR_w(\lambda_i))}{\ln(nR_w(\lambda_j))} - m_0 \qquad (2)$$

where, Z = the depth; Rw (ƛi) and Rw (ƛj) = atmospherically corrected pixel value for Blue (i) and Green (j) respectively. m1, m0= offset and gain determined empirically, n= the fixed constant ensuring a positive value after the log transform and a linear response between the ratio and the depth. In this model, two parameters (m0 and m1) need to be estimated by performing linear regression analysis between measured Z value from field survey and to get m0 and m1 value from Landsat image analysis. In this study, visual interpretation and manual digitization of river bank lines of the different years were made to assess the erosion and deposition of Karnaphuli River. There were total 21 observation points for the measured depth (Figure 2). These are the locations of erosion and depositions were identified from the Landsat imagery during 1978 and 2018 using ArcMap ver. 10.5.

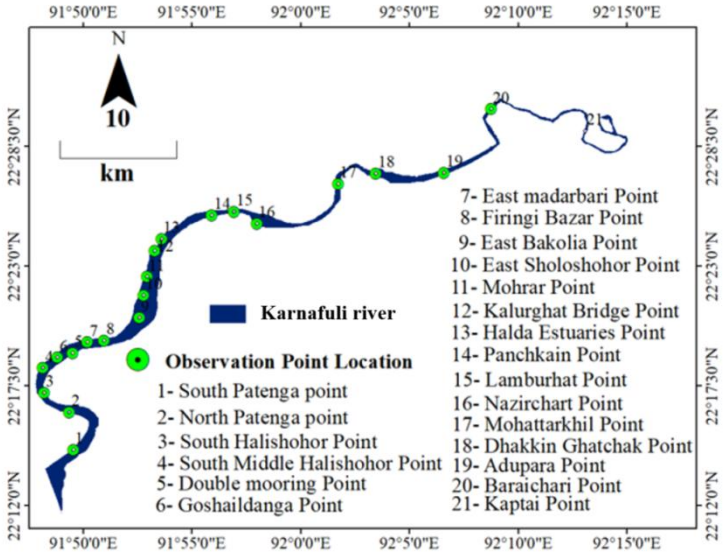

Figure 2. Observation point location map.

R2 value was computed using the following equations:

$$R^2 = \frac{n\left(\sum_{m=1}^{n} Z(F)\right) - \left(\sum_{m=1}^{n} Z_m\right)\left(\sum_{m=1}^{n}(F)\right)}{\sqrt{\left[n\sum_{m=1}^{n}\left(\sum_{m=1}^{n}(F) - \left(\sum_{m=1}^{n} F\right)^2\right)\right]\left[\left(n\sum_{m=1}^{n} Z^2\right) - \left(\sum_{m=1}^{n} Z^2\right)\right]}} \qquad (3)$$

Where, F = $\left|R_{wmi} - R_{wmj}\right|$
n = number of points
R_{wmi} = Blue band value at point m
R_{wmj} = Green band value at point m

5 RESULTS AND DISCUSSIONS

The Karnaphuli river bathymetry map for the years 1978, 1985, 1999, 2011, and 2018 derived from Landsat imagery using the Stumpf model (Figure 3). The water depth points and the corresponding pixel value of the Landsat image were obtained. The depth range was from -3m to 6m. Thus, the changes in bed level of the Karnaphuli river was estimated from 1978 to 2018 using Landsat image analysis (Figure 3). Year-wise bed elevation ranges for the different locations are noted from the Landsat image analysis (Table 2).

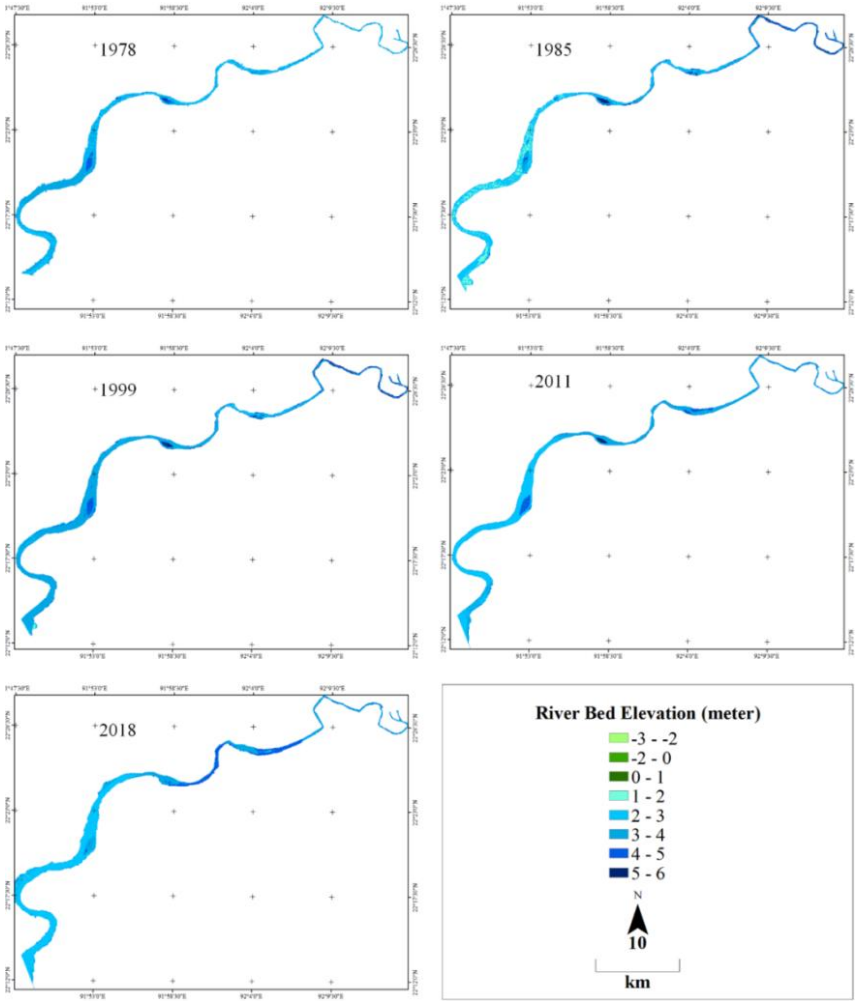

Figure 3. River bed elevation over the period.

Table 2. Riverbed elevation observation using Landsat image analysis.

Year	Bed Elevation Range for different Location	
	-3m – 3m	3m – 6m
1978	South Patenga Ward, North Patenga, SouthHalishahar, East Sholoshohor, Mohra, Kalur Ghat Bridge, Panchkain, Lamburhat, Mohattarkhil, Dhakkinghatchak.	South Middle Halishahar, Double mooring, Goshaildanga, East Madar Bari, Firingi Bazar, East Bakolia, Halda Estuaries, Nazirchar,AduparaBaraichari
1985	SouthPatenga, North Patenga, South Halishahar, South Middle Halishahar, Double mooring, East Sholoshohor, Kalur Ghat Bridge, Panchkain, Firingi Bazar, Halda Estuaries.	Mohra, Lamburhat, Mohattarkhil, Dhakkinghatchak, East Bakolia, Nazirchar, Adupara, Baraichari.
1999	KalurGhat Bridge, Lamburhat,Mohattarkhil, South Middle Halishahar, Goshaildanga.	SouthPatenga, North Patenga, South Halishahar, East Sholoshohor, Mohra Point, Double mooring, East Madar Bari, Firingi Bazar, EastBakolia, Panchkain, Dhakkinghatchak, Halda Estuaries, Nazirchar, Adupara, Baraichari.
2011	South Patenga, North Patenga Point, South Halishahar, East Sholoshohor, Mohra, Kalur Ghat Bridge, South Middle Halishahar, Double mooring, Goshaildanga, Halda Estuaries.	Panchkain, Lamburhat, Mohattarkhil, Dhakkinghatchak, East Madar Bari,Firingi Bazar, East Bakolia, Nazirchar,Adupara point, Baraichari.
2018	South Patenga, North Patenga, Mohra, South Halishahar, Double mooring, Goshaildanga, East Madar Bari, East Sholoshohor, KalurGhat Bridge point.	Panchkain, Lamburhat, Dhakkinghatchak, South Middle Halishahar, Firingi Bazar, East Bakolia, Halda Estuaries, Nazirchar, Adupara point, Baraichari.

From the imagery processing, a decreased deposition on bed has found in seven locations i.e. South Patenga, North Patenga, South Halishahar, East Sholoshohor, Mohra Point, Double mooring, and Halda Estuaries after 1999 compare to 1985. Although, Halda Estuaries showed a variability in erosion and deposition throughout the study period. The output of the executed process is compared to the measured depth at all the 21 observation points using eco sounder, and corresponding pixels values that are estimated water depth from Landsat imagery were obtained for 2018. R2 value was computed between measured and estimated water depth for the model validation using Eq. 3 (Figure 4).

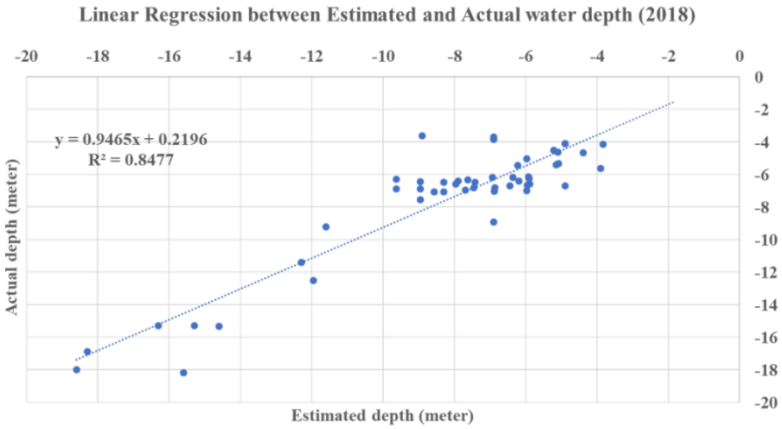

Figure 4. Correlation between estimated and actual water depth.

A representative cross-section for each observation location of the Karnaphuli river was prepared by creating a profile graph using ArcMap Software version 10.5 and an example for observation point 9 (East Bakolia) has presented in Figure 5.

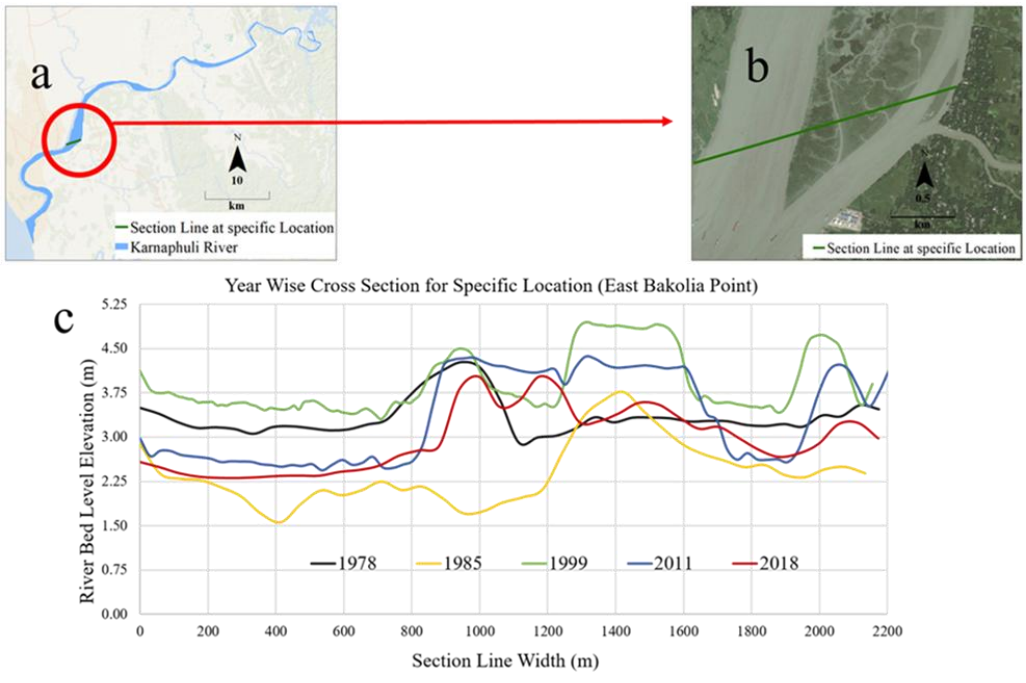

Figure 5. River cross-section at East Bakolia point.

The erosion and deposition area of the Karnaphuli river from 1978 to 2018 are depicted (Figure 6). The erosion area is larger than the deposition area over the study period. Karnaphuli river experienced increased erosion after the year of 1990 and an increasing trend persists in due course (Figure 7). The acquired bathymetry showed erosion and deposition within the Karnaphuli river at a rate of 263000m^2/year and 55000m^2/year respectively.

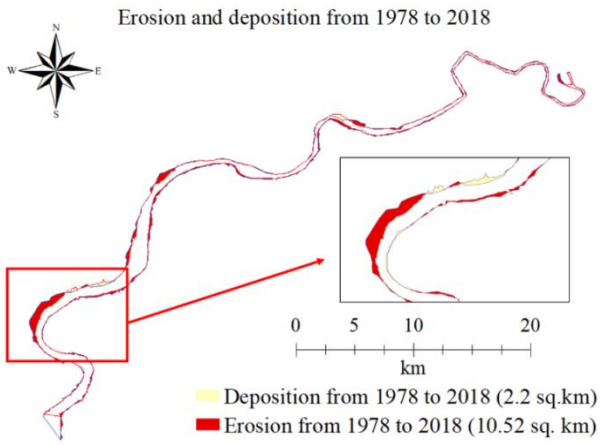

Figure 6. Erosion and deposition of Karnaphuli river.

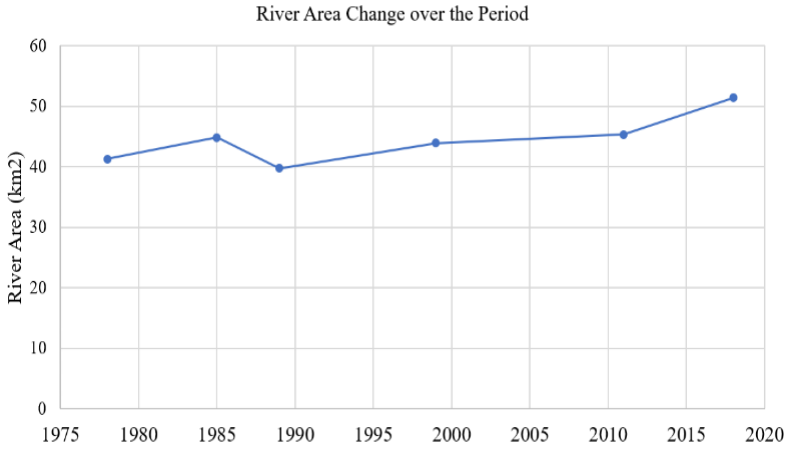

Figure 7. River area over the period.

6 CONCLUSIONS

This study aimed to conduct a satellite-derived bathymetry mapping to mimic the field-based maps. The calibrated parameters m1 and m0 in the Stumpf model were estimated for 1978 and 1988 and applied to 1999 and 2018.From 1978 to 2018, the application could reasonably represent the river water depth while processes Landsat images. With proper field survey data, on river morphology, land use changes and hydraulic structures in due courses, this approach could be applicable to provide details guidance for any existing and proposed hydraulic structures. Thus, could be a cost effective approach for any river engineering works.

REFERENCES

Abd-almajied, M. I. (2015) 'Predicting Water Depth of Lake Using Remote Sensing image', *Iraqi journal of science*, 56(2), pp. 1208–1215.

Baban, S. M. J. (1993) 'The evaluation of different algorithms for bathymetric charting of lakes using Landsat imagery', *International Journal of Remote Sensing*, 14, pp. 2263–2273.

Benny, A. H. and Dawson, G. (1983) 'Satellite Imagery as an Aid to Bathymetric Charting in the Red Sea', *The cartographic Journal*, 20(1)(March), pp. 5–16. doi: 10.1179/caj.1983.20.1.5.

Cracknell, A. P. and Ibrahim, M. (1988) 'Bathymetry studies on the coastal waters (Red Sea) of Jeddah , Saudi Arabia , using Shuttle MOMS-01 data', *International Journal of Remote Sensing*, 9:6, pp. 1161–1165. doi: 10.1080/01431168808954923.

Deng, Z., Ji, M. and Zhang, Z. (1979) 'Mapping bathymetry from multi-source remote sensing images: a case study in the Beilun Estuary , Guangxi , China', in *The International Archives of the Photogrammetry, Remote Sensing and Spatial Information Sciences. Vol. XXXVII. Part B8. Beijing 2008 photochemistry*, pp. 1321–1326.

Duplančić, T., Leder, N. and Peroš, J. (2019) 'Satellite Derived Bathymetry Survey Method – Example of Hramina Bay', *Transations ans maritime science*, 10, pp. 99–108. doi: 10.7225/toms.v08.n01.010.

El-sayed, M. S. (2018) 'Comparative Study of Satellite Images Performance in Mapping Lake Bathymetry : Case Study of Al-Manzala', *American Journal of Geographic Information System*, 7(3), pp. 82–87. doi: 10.5923/j.ajgis.20180703.02.

Jawak, S. D., Raut, D. A. and Luis, A. J. (2015) 'Iterative Spectral Index Ratio Exploration for Object-based Image Analysis of Antarctic Coastal Oasis Using High Resolution Satellite Remote Sensing Data', *Aquatic Procedia*. Elsevier B.V., 4(Icwrcoe), pp. 157–164. doi: 10.1016/j.aqpro.2015.02.022.

Lyzenga, D. R. (1978) 'Passive remote sensing techniques for mapping water depth and bottom features', 17(3), pp. 379–383.

Lyzenga, D. R., Malinas, N. P. and Tanis, F. J. (2006) 'Multispectral Bathymetry Using a Simple Physically Based Algorithm', 44(8), pp. 2251–2259.

Pushparaj, J. and Hegde, A. V. (2017) 'Estimation of bathymetry along the coast of Mangaluru using Landsat-8 imagery', *International journal of ocean and climate system*, 8(2), pp. 71–83. doi: 10.1177/1759313116679672.

Stumpf, R. P. *et al.* (2003) 'Determination of water depth with high-resolution satellite imagery over variable bottom types', *American Society of limonology and oceonography*, 48, pp. 547–556.

Su, H., Liu, H. and Heyman, W. D. (2014) 'Automated Derivation of Bathymetric Information from Multi-Spectral Satellite Imagery Using a Non-Linear Inversion Model', *Marine Geodesy*, (August 2014), pp. 37–41. doi: 10.1080/01490410802466652.

Tripathi, N. K. and Rao, A. . (2002) 'Bathymetric mapping in Kakinada Bay , India , using IRS-1D LISS-III', *International Journal of Remote Sensing*, 23:6, pp. 1013–1025. doi: 10.1080/01431160110075785.

Winterbottom, S. J. and Gilvear, D. J. (1997) 'Quantification of channel bed morphology in gravel-bed rivers using airborne multispectral imagery and aerial photography', *Research and management*, 13(June), pp. 489–499.